







Original Research

# Functional Heterogeneity of Hepatitis B Virus-Specific CD8<sup>+</sup> T Cells Mediates the Clinical Outcomes of Infection

Zhijun Shen<sup>1,2</sup>, Xin Wang<sup>1</sup>, Juan Zhao<sup>1</sup>, Mi Wu<sup>1</sup>, Ting Zhou<sup>1</sup>, Lichen Ouyang<sup>3</sup>,  
 Xiufang Weng<sup>1</sup>, Shiguo Liu<sup>2,\*</sup>, Xiongwen Wu<sup>1,\*</sup>

<sup>1</sup>Department of Immunology, School of Basic Medicine, Tongji Medical College, Huazhong University of Science and Technology, 430030 Wuhan, Hubei, China

<sup>2</sup>Department of Clinical Laboratory, Hubei No.3 People's Hospital of Jiangnan University, 430033 Wuhan, Hubei, China

<sup>3</sup>Department of Immunology, School of Medicine, Jiangnan University, 430056 Wuhan, Hubei, China

\*Correspondence: [lsgg518@163.com](mailto:lsgg518@163.com) (Shiguo Liu); [xiongwenwu@hotmail.com](mailto:xiongwenwu@hotmail.com) (Xiongwen Wu)

Academic Editor: Sukmook Lee

Submitted: 3 March 2026 Revised: 19 April 2026 Accepted: 29 April 2026 Published: 21 May 2026

## Abstract

**Background:** Hepatitis B virus (HBV)-specific CD8<sup>+</sup> T cells play a crucial role in viral clearance. However, in patients with chronic hepatitis B infections, sustained immune activation leads to functional impairment of these HBV-specific CD8<sup>+</sup> T cells. The goal of this study was to clarify whether these virus-specific CD8<sup>+</sup> T cells are exhausted or reflect an incomplete response derived from the initial T cell repertoire. **Methods:** In this study, HBV core 18–27 epitope-specific CD8<sup>+</sup> T cells were identified by proliferation through *in vitro* antigen stimulation. Peptide-specific CD8<sup>+</sup> T cells recognizing the cytomegalovirus (CMV) pp65 495–503 epitope were used as a positive control, as they exhibit a robust immune response. Single-cell sequencing was employed to characterize the TCR repertoire of expanded clones. Correlations between T cell subsets and clinical outcomes were analyzed and compared. **Results:** Both HBV core 18–27-specific and CMV pp65-specific CD8<sup>+</sup> T cells were successfully classified into three functionally distinct subsets: IFN $\gamma$ <sup>+</sup>, mTGF $\beta$ <sup>+</sup>, and IFN $\gamma$ <sup>-</sup>/mTGF $\beta$ <sup>-</sup>. Those patients with resolved acute HBV infections and HBV core 18–27 specific CD8<sup>+</sup> T cells exhibited the highest IFN $\gamma$ <sup>+</sup>/mTGF $\beta$ <sup>+</sup> ratio, reaching levels comparable to those of CMV pp65-specific CD8<sup>+</sup> T cells. Inactive HBV carriers exhibited the second-highest IFN $\gamma$ <sup>+</sup>/mTGF $\beta$ <sup>+</sup> ratio, while this ratio was lowest among patients exhibiting viral immune tolerance. HBV core 18–27 tetramer staining and ERGO-II Model prediction demonstrated that IFN $\gamma$ <sup>+</sup> subset CD8<sup>+</sup> T cells exhibited the highest affinity for this epitope, followed by the mTGF $\beta$ <sup>+</sup> subset, with IFN $\gamma$ <sup>-</sup>/mTGF $\beta$ <sup>-</sup> cells exhibiting the lowest affinity. **Conclusions:** These results suggest that individuals with a high IFN $\gamma$ <sup>+</sup>/mTGF $\beta$ <sup>+</sup> ratio exhibit a lower HBV viral load. The IFN $\gamma$ <sup>+</sup>/mTGF $\beta$ <sup>+</sup> CD8<sup>+</sup> T cell ratio, in particular, appears to be associated with HBV clearance, and this may be attributable to T cell receptor affinity for HBV epitopes.

**Keywords:** chronic hepatitis B; viral load; cell proliferation; immune tolerance; CD8-Positive T-Lymphocytes; T-cell receptor diversity; ligand-receptor interactions; TCR affinity

## 1. Introduction

Chronic hepatitis B infection (CHB) remains a global public health problem. According to the World Health Organization, approximately 2 billion people worldwide have been infected with the hepatitis B virus (HBV), of whom 254 million people are chronically infected [1]. Annually, about 1.1 million deaths are attributable to HBV-related complications, including liver failure, cirrhosis, and hepatocellular carcinoma. In China, the “Guidelines for the Prevention and Treatment of Chronic Hepatitis B (2022 Edition)” reported that HBV affects approximately 6.1% of the general population, corresponding to roughly 86 million cases of HBV infection, including 20–30 million cases of CHB [2].

HBV-specific CD8<sup>+</sup> T cells play a crucial role in viral clearance [3]. However, in patients with CHB, the immune system fails to eliminate the virus effectively. The prevailing evidence suggests that HBV-specific CD8<sup>+</sup> T cells exist in a state of prolonged immune activation in CHB patients,

leading to their dysfunction and exhaustion [4]. Individual patients exhibit heterogeneous HBV peptide-specific CD8<sup>+</sup> T cell responses, and this variability has been attributed to multiple factors, including differences in epitopes and antigen-presenting cells (APCs) [5]. The responsiveness of T cells for specific HBV epitopes also differs markedly. For instance, relative to HBV pol455–463 epitope-specific CD8<sup>+</sup> T cells, HBV core 18–27 epitope-specific CD8<sup>+</sup> T cells exhibit higher frequencies and more robust immune functionality, including higher levels of IFN $\gamma$ , TNF- $\alpha$ , and CD107a expression [6]. Although there is also variability in the immune responsiveness of individuals with the different human leukocyte antigen (HLA) subtypes [7], this fails to account for the differential immune responses observed among individuals with the same HLA subtype.

In an effort to more fully clarify the immunological basis for inconsistent HBV-specific immunity, we hypothesized that specific CD8<sup>+</sup> T cells recognizing a single peptide-major histocompatibility complex (pMHC) com-



plex may differ in their responsiveness such that they can be classified based on their activity into subsets with effective, inhibitory, and hyporeactive responsiveness. T cell repertoire heterogeneity is currently considered to be the principal driver of observed differences in viral clearance, whereas T cell exhaustion is thought to be a relatively minor contributing factor. Differences in T cell reactivity are epitope-specific. For example, in the context of cytomegalovirus (CMV) infection, a diverse T cell repertoire enables robust and effective immunity, whereas in CHB infection, the repertoire is often dominated by hyporeactive or inhibitory T cell subsets, leading to an impaired immune response and poor viral clearance [7].

Research focused on the tumor microenvironment has informed the classification of hyporeactive T cells into three categories: exhausted T cells, arising from persistent antigen stimulation; anergic T cells, which lack the first or second signals; and senescent T cells, which are functionally intact but possess limited replicative potential [8]. The common defining characteristic of these three subsets is low proliferative capacity. However, further research is warranted to investigate the presence of these types of T cells in CHB and to clarify how they influence the immune response. As such, proliferation was selected as a core criterion to evaluate T cell specificity in the present study based on analyses of the responsiveness of T cells specific to a single pMHC.

Prior studies of peptide-specific CD8<sup>+</sup> T cells have primarily relied on the use of pMHC tetramers or multimers for detection. However, due to low precursor frequencies, these antigen-specific CD8<sup>+</sup> T cells are often undetectable or are inaccurately quantified. Although tetramer-associated magnetic enrichment (TAME) has been developed to improve detection accuracy [9], it may still fail to detect some low-affinity cells. Given this limitation, pMHC tetramer staining was used in this study not as a definitive indicator of T cell specificity, but rather as a means of assessing relative pMHC-TCR affinity.

The primary aims of this study were to investigate the differentiation of HBV-specific CD8<sup>+</sup> T cells in CHB, and to examine the functional heterogeneity of clonotypes targeting a single pMHC. Through an *in vitro* culture approach, proliferated T cells were identified as specific CD8<sup>+</sup> T cells, enabling the further assessment of their functional profiles. Additionally, tetramer staining was used to identify highly reactive specific CD8<sup>+</sup> T cells. The relationship between pMHC-TCR affinity and the differentiation of specific CD8<sup>+</sup> T cells was investigated, based on the hypothesis that viral persistence in CHB may be driven in part by the absence of hyporeactivity of specific CD8<sup>+</sup> T cells in certain patients. Based on our previous identification of an inhibitory CD8<sup>+</sup> T cell subpopulation characterized by high expression of membrane-bound TGF $\beta$  (mTGF $\beta$ ) among alloreactive T cells [10], we speculated that a similar mTGF $\beta$ <sup>+</sup> subpopulation may exist in some

HBV patients. Accordingly, in this study, T cells expressing IFN $\gamma$  were identified as the effective subset (IFN $\gamma$ <sup>+</sup>), while those expressing mTGF $\beta$  were classified as the inhibitory subset (mTGF $\beta$ <sup>+</sup>), and those expressing neither of these markers were classified as the hyporeactive subset (IFN $\gamma$ <sup>-</sup>/mTGF $\beta$ <sup>-</sup>).

CHB infection provides a valuable natural model for studying specific T cell responses. Developing a deeper understanding of the functional diversity among specific CD8<sup>+</sup> T cells will help elucidate the mechanisms of viral persistence while also informing the development of novel T cell-based immunotherapies.

## 2. Materials and Methods

### 2.1 Preparation of Clinical Samples

Patients were recruited at Hubei No.3 People's Hospital of Jiangnan University. All patients had HBV infection and tested negative for hepatitis A, C, and D viruses, and HIV. The detailed clinical characteristics for these patients are presented in **Supplementary Table 1**. Most of these patients were undergoing long-term nucleos(t)ide analogue (NA) therapy, such as tenofovir disoproxil fumarate (TDF) and tenofovir alafenamide (TAF); notably, none had received interferon therapy. Furthermore, no liver fibrosis was detected in any of the included cases, thereby minimizing potential confounding effects on T cell phenotypes and functions.

Individuals were categorized into three groups: immune tolerance-stage patients (IT group, n = 16), defined as those with HBV DNA >20,000 copies/mL, alanine aminotransferase (ALT) <40 U/L, hepatitis B surface antigen positive (HBsAg<sup>+</sup>), hepatitis B e-antigen positive (HBeAg<sup>+</sup>); inactive carrier patients (IC group, n = 30), defined as HBV DNA <2000 copies/mL or undetectable, ALT <40 U/L, HBsAg<sup>+</sup>, HBeAg<sup>-</sup>; and acute resolved patients (R group, n = 14), defined as having an undetectable HBV DNA load, HBsAg<sup>-</sup>, anti-HBcAb<sup>+</sup>. For each participant, up to 5 mL of heparin-anticoagulated blood was obtained, and peripheral blood mononuclear cells (PBMCs) were isolated by Ficoll density gradient centrifugation. Then, PBMCs were resuspended in X-VIVO® 15 medium (Cat. No.: BE02-060Q, Lonza, Basel, Switzerland) containing 5% human AB serum (off the clot) (Cat. No.: S-HUO-US-011, SERANA Europe GmbH, Pessin, Brandenburg, Germany), followed immediately by subsequent experiments to ensure cell viability. A total of 99 HLA-A2<sup>+</sup> HBV-infected individuals were screened. After excluding non-expanded and non-specifically expanded samples, 60 individuals with detectable HBV-specific CD8<sup>+</sup> T cells were included.

### 2.2 Peptides and Tetramers

Epitope-specific peptides were synthesized by Sino Biological Inc. (Shanghai, China). These included the HBV core 18–27 wild-type (FLPSDFFPSV), HBV core 18–27 mutant (FLPSDFFPSI), and CMV pp65 495–503

(NLVPMVATV) epitopes. All peptides were desalted and obtained with a purity greater than 99%. The HBV core 18–27 (FLPSDFFPSV) HLA A\*02:01 tetramer (Tet-HBC) was ordered from Medical & Biological Laboratories Co., Ltd. (Cat. No.: TB-0018-2, MBL, Minato-ku, Tokyo, Japan).

### 2.3 Flow Cytometry and Cell Identity Verification

All antibodies were ordered from BioLegend (San Diego, CA, USA) and included the following: FITC anti-human HLA-A2 (BB7.2 clone), APC/Cy7 anti-human CD3 (UCHT1 clone), PE/Cy5 anti-human CD8a (HIT8a clone), and PE anti-human LAP (TGF- $\beta$ 1) (TW4-6H10 clone). The Tag-it Violet™ Proliferation and Cell Tracking Dye (CellTrace) (Cat. No.: 425101, BioLegend, San Diego, CA, USA) was used in this study. Cells were washed with phosphate-buffered saline (PBS), pelleted, incubated with tetramer for 1 h at 4 °C, and then stained with surface antibodies (1:1000) for 30 min at 4 °C. The utilized gating strategy was outlined in **Supplementary Fig. 1A**.

All primary cells from clinical samples were validated for their identity via surface marker staining (CD3/CD8/HLA-A2) using flow cytometry. The T2 cell line was identified by specific HLA-A2 antibody (BB7.2 clone) staining (**Supplementary Fig. 1B**) and validated by STR profiling. All cell preparations were tested and confirmed to be negative for mycoplasma contamination.

### 2.4 In Vitro Expansion of Peptide-Specific CD8+ T Cells

PBMCs were stained with CellTrace (20 mM, 1:2000), then adjusted to  $1\text{--}2 \times 10^6$  cells/mL and cultured with X-VIVO® 15 medium containing 5% human AB serum in 24-well plates. Epitope-specific peptides (40  $\mu$ g/mL) and monoclonal anti-CD28 antibody (1  $\mu$ g/mL, Cat. No.: 555725, BD Biosciences, San Jose, CA, USA) were added on Day 0. Half the medium was exchanged on Days 2, 7, and 9, along with the addition of rIL-2 (50 IU/mL, Cat. No.: 130-097-748, Miltenyi Biotec Inc., Auburn, CA, USA). Expanded cells were analyzed on Day 10 or Day 11, depending on cell state. Non-specific expansion will be strictly eliminated.

### 2.5 Functional Assays Using Peptide-Specific CD8+ T Cells

To provide sustained continuous stimulation of all specific CD8+ T cells, T2 cells were used as APCs. T2 cells were cultured in RPMI-1640 (Cat. No.: 21875034) supplemented with 10% fetal bovine serum (Cat. No.: 10099-141) (both from Gibco, Thermo Fisher Scientific, Waltham, MA, USA). Before re-stimulation, both T2 cells and expanded cells were transitioned into X-VIVO® 15 medium. T2 cells were adjusted to  $1\text{--}2 \times 10^6$  cells/mL and incubated with epitope-specific peptides (40  $\mu$ g/mL) overnight. The peptide-loaded T2 cells were then cocultured with expanded cells at an effector/target ratio of 1:1–1:2 for 4–6 h. Staphylococcal enterotoxin B (SEB) (1  $\mu$ g/mL, Cat. No.:

PT405, Toxin Technology, Sarasota, FL, USA) was used as a positive control. To ensure expanded cells were viable for subsequent use, an IFN $\gamma$  Secretion Assay-Det. Kit (FITC) (Cat. No.: 130-090-524, Miltenyi Biotec Inc., Auburn, CA, USA) (antibody capture) was used to detect IFN $\gamma$ + T cells according to the manufacturer's protocol. In the blocking assay, a purified antihuman/mouse TGF $\beta$ 1 antibody (1  $\mu$ g/mL, Clone: 19D8, BioLegend, San Diego, CA, USA) was added during the re-stimulation of expanded cells.

### 2.6 Single-Cell Immune-Targeted mRNA Sequencing and TCR Sequencing

Cells from different samples were labeled with Human Single-Cell Multiplexing Kit (Sample Tags) (Cat. No.: 633793, BD Biosciences, San Jose, CA, USA), and subsequently sorted by flow cytometry (FACS AriaII, BD Biosciences) to isolate those cells with aCD3+/CD8+/CellTrace<sup>dim</sup> phenotype. The sorted cells from each sample were pooled in equal quantities for subsequent single-cell analysis. Single-cell capture and RNA library preparation were performed using the BD Rhapsody™ system according to the manufacturer's protocol. Single-cell immune-targeted RNA sequencing was performed on a Novaseq 6000 System (Illumina Inc., San Diego, CA, USA) to profile the expression of 400 immune-associated genes through Immune Response Panel Hs Kit (Cat. No.: 723770, BD Biosciences, San Jose, CA, USA). A total of 7 CHB patient samples were processed, yielding 4638 single-cell transcriptomes after pipeline analysis. KEGG enrichment analyses were performed among the IFN $\gamma$ +, mTGF $\beta$ +, and IFN $\gamma$ -/mTGF $\beta$ - subsets. For T cell receptor (TCR) sequencing, paired-end sequencing (PE250) was employed to ensure 500 bp reads covering the CDR3 region, enabling reliable identification of different T-cell receptor alpha variable region (TRAV) and T-cell receptor beta variable region (TRBV).

### 2.7 TCR-pMHC Affinity Prediction Using ERGO-II Models

The ERGO-II (pEpitide tCR matchinG predictiOn) model [11] is a multifactorial TCR-pMHC binding predictor (<https://github.com/IdoSpringer/ERGO-II>). This model is based on the long short-term memory (LSTM) model. Utilized input factors included: amino acid sequences of the CDR3 region in TRAV and TRBV; peptide amino acid sequences; and TRAV, TRBV, TRAJ, TRBJ, and MHC subtypes. VDJdb was used as a training database. Final scores were used to reflect TCR-pMHC affinity. The 10 most frequent representative clones were chosen from among the IFN $\gamma$ +, mTGF $\beta$ +, and IFN $\gamma$ -/mTGF $\beta$ - subsets, with higher final scores indicating greater TCR-pMHC affinity.

### 2.8 Data Analysis

For flow cytometric gating, an initial peptide-specific CD8+ T cell gate was set based on side scat-

ter (SSC)/forward scatter (FSC) and subsequent gating on single-cells (FSC-A/FSC-H), CD3<sup>+</sup>, and CD8<sup>+</sup>, CellTrace<sup>dim</sup> gates, followed by the introduction of IFN $\gamma$ <sup>+</sup> and mTGF $\beta$ <sup>+</sup> gates. FlowJo (BD, 10.5.3) was used to analyze flow cytometry data. After sequencing, raw data were transferred to visual Excel matrices using the BD Rhapsody™ Targeted Analysis Pipeline (<https://velsera.com/bd-rhapsody/>). For single-cell immune-targeted RNA sequencing, R (1.41.1717.0) was used for KEGG enrichment analysis, Gene Set Enrichment Analysis (GSEA), and heatmap analysis of immune-related genes. For single-cell TCR sequencing, the VDJ Explorer module in the SeqGeq software (v1.8, BD Biosciences, San Jose, CA, USA) was used to analyze TCR diversity. By aligning to the GRCh38 reference genome, this module can display the amino acid sequence and length of the CDR3 region, as well as dominant clonotypes with paired TRAV/TRBV.

### 2.9 Statistical Analyses

As most quantitative data in this study were not normally distributed, nonparametric tests were used. For comparisons between two matched-pair groups, Wilcoxon tests were used, while for comparisons among three groups, the Friedman test (matched-pairs) or the Kruskal-Wallis test (no matched-pairs) was used, followed by Dunn's multiple comparisons test. Quantitative data that were normally distributed were analyzed with one-way ANOVAs and Tukey's multiple comparisons test when comparing results among three groups.  $p < 0.05$  was considered statistically significant. Those analyses were all performed in GraphPad Prism (9.5.0, GraphPad Software, San Diego, CA, USA). Additionally, the Kolmogorov-Smirnov test was used for GSEA analysis and performed in R (1.41.1717.0, R Foundation for Statistical Computing, Vienna, Austria).

## 3. Results

### 3.1 In Vitro Expansion Enables HBV-Specific CD8<sup>+</sup> T Cell Subset Identification

HBV-specific CD8<sup>+</sup> T cells targeting the HLA-A2-restricted core 18–27 HBV epitope were expanded *in vitro* (Fig. 1A). The utilized epitopes included both wild-type FLPSDFFPSV (HBC group) and the mutant variant FLPSDFFPSI (HBC-PSI group). CMV-specific CD8<sup>+</sup> T cells targeting the HLA-A2-restricted pp65 495–503 epitope were used as a positive control (CMV group). Samples showing nonspecific or no expansion were excluded from further analysis.

The HBC group exhibited a lower expansion rate compared to the CMV group, while no significant difference was observed between the HBC and HBC-PSI groups (Fig. 1B). The final expanded cell count varied substantially across individuals, as it was largely determined by the precursor frequency of specific T cells in each donor. With an initial total cell concentration of  $1\text{--}2 \times 10^6$  cells/mL, the yield ranged from 5000 to 100,000 cells/mL in the

CMV group, and from 100 to 2000 cells/mL in both the HBC and HBC-PSI groups. Both the HBC group and the HBC-PSI group were detectable using the HBV core 18–27 tetramer (Tet-HBC) (**Supplementary Fig. 2A**), and HBV core 18–27 specific CD8<sup>+</sup> T cells expanded with the wild-type peptide (HBC) were able to secrete IFN $\gamma$  upon re-stimulation with T2 cells presenting the mutant peptide (T2-HBC-PSI) (**Supplementary Fig. 3A**). Therefore, only the HBC group was selected for use in subsequent analyses. The proliferation rate was also found to be proportional to the rate of Tet-HBC positivity ( $R^2 = 0.4417$ ,  $p = 0.0010$ , Fig. 1C), consistent with specific CD8<sup>+</sup> T cell expansion. Notably, Tet-HBC<sup>+</sup> T cells were only partially detected within the CellTrace<sup>dim</sup> subset, highlighting the limitations of tetramer-based detection of specific CD8<sup>+</sup> T cells. Consequently, the CellTrace<sup>dim</sup> subset indicative of proliferated cells was used to identify epitope-specific CD8<sup>+</sup> T cells.

After *in vitro* expansion, HBV-specific CD8<sup>+</sup> T cells were re-stimulated with peptide-loaded T2 cells and assessed for IFN $\gamma$  and mTGF $\beta$  expression through functional assays (Fig. 1D). SEB, which was used as a nonspecific stimulant in these assays, elicited high rates of IFN $\gamma$  positivity in both the proliferated subset (CellTrace<sup>dim</sup>) and the non-proliferated subset (CellTrace<sup>+</sup>) (**Supplementary Fig. 3B**). These results indicate that different phenotypic subsets can be induced by a single peptide. CellTrace mean fluorescence intensity (MFI) reflects the extent of cell proliferation. In this experiment, the IFN $\gamma$ <sup>+</sup>, mTGF $\beta$ <sup>+</sup>, and IFN $\gamma$ <sup>−</sup>/mTGF $\beta$ <sup>−</sup> T cell subsets exhibited differing CellTrace MFI values (Fig. 1E). The proliferation pattern of mTGF $\beta$ <sup>+</sup> cells was similar to that of IFN $\gamma$ <sup>+</sup> cells, but the frequency of mTGF $\beta$ <sup>+</sup> cells was low, likely owing to their low precursor frequency. According to previous studies [10], this subset exhibits strong inhibitory activity, and it was thus selected as a representative marker of the inhibitory subset.

To functionally validate this mTGF $\beta$ <sup>+</sup> subset, an anti-TGF $\beta$  antibody was introduced during stimulation. We observed a significant increase in IFN $\gamma$ <sup>+</sup> frequency in the group stimulated with HBC and treated with anti-TGF $\beta$  as compared to the HBC group (Fig. 1F). This indicated that the mTGF $\beta$ <sup>+</sup> T cell subset has an inhibitory effect on T cell responses, with differing T cell phenotypes corresponding to distinct T cell functionality. These results show that single peptide-specific CD8<sup>+</sup> T cells comprise different functional subsets that can be distinguished based on IFN $\gamma$  and mTGF $\beta$  expression, including an effector subset expressing IFN $\gamma$  (IFN $\gamma$ <sup>+</sup>), an inhibitory subset expressing mTGF $\beta$  (mTGF $\beta$ <sup>+</sup>), and a hyporeactive subset expressing neither IFN $\gamma$  nor mTGF $\beta$  (IFN $\gamma$ <sup>−</sup>/mTGF $\beta$ <sup>−</sup>).

### 3.2 CD8<sup>+</sup> T Cell Subsets Differ in Terms of Recognition, Activation, Differentiation, and Effect Stage

To further clarify the biological functions of these different functional subsets, HBV-specific CD8<sup>+</sup> T cells were subjected to single-cell immune-targeted RNA sequencing.

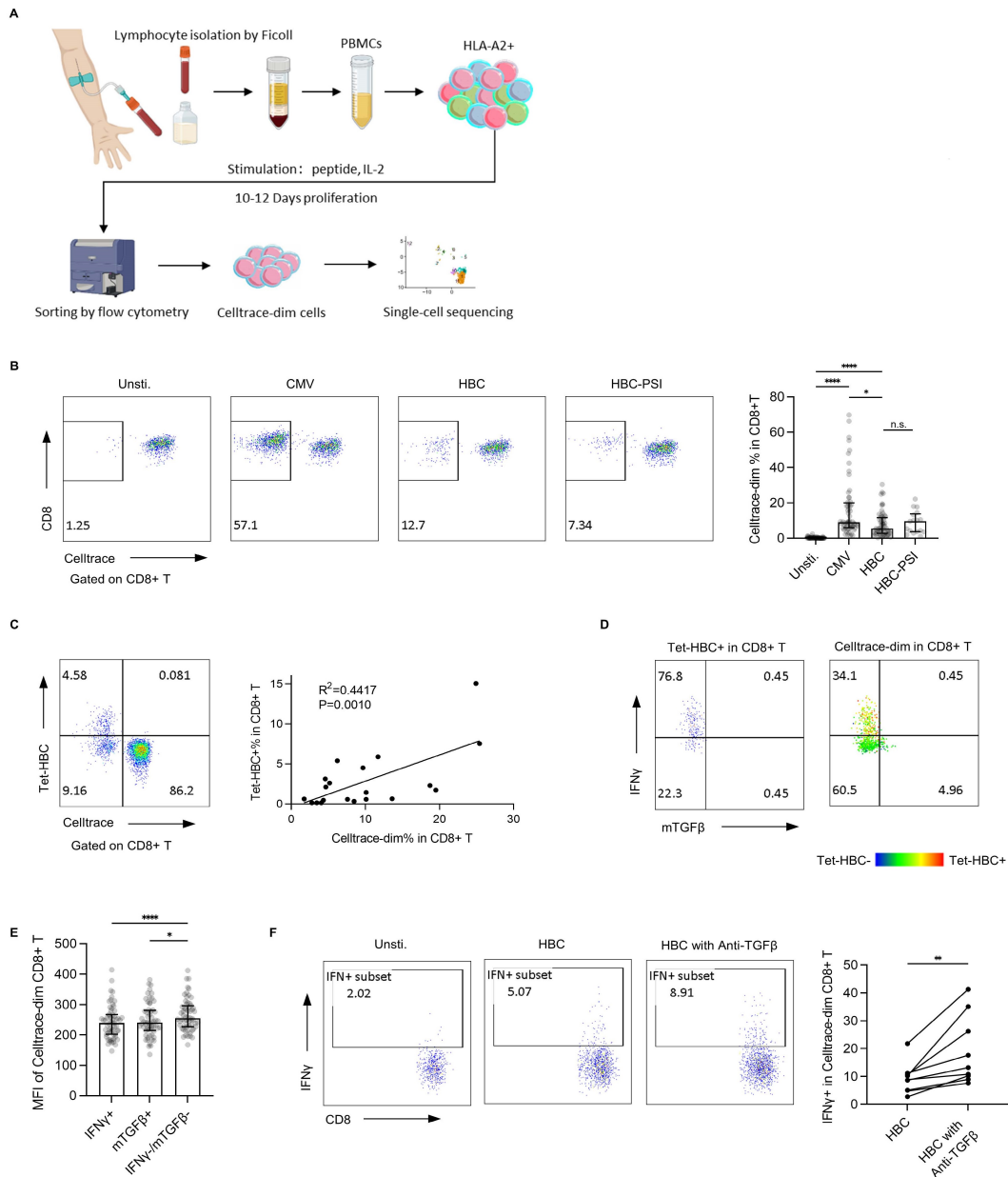


**Fig. 1. *In vitro* expansion of single peptide-specific CD8+ T cells.** (A) Study flowchart. (B) The percentage of proliferated cells after *in vitro* expansion was assessed by flow cytometry. Left panel: representative plot from one patient with a chronic hepatitis B infection. Right panel: bar plot for all samples (Unstimulated, CMV, HBC: n = 60, HBC-PSI: n = 17), with the bar showing the median and interquartile range. (C) HBV core 18–27 tetramer-based detection of CD8+ T cells. Left panel: a representative tetramer detection plot. Right panel: Linear regression analysis of the association between Tet-HBC+ cells and CellTrace<sup>dim</sup> cells. (D) IFN $\gamma$  and mTGF $\beta$  expression on Tet-HBC+ cells and CellTrace<sup>dim</sup> cells (n = 21). (E) The MFI of CellTrace<sup>dim</sup> CD8+ T cells in IFN $\gamma$ +, mTGF $\beta$ +, and IFN $\gamma$ -/mTGF $\beta$ - subset. (F) IFN $\gamma$  expression in the Unstimulated, HBC, and HBC + anti-TGF $\beta$  groups of CellTrace<sup>dim</sup> cells after sorting by flow cytometry (n = 9). Left panel: representative plot. Right panel: plot showing the HBC and HBC + anti-TGF $\beta$  groups. Unsti., Unstimulated group; CMV, Cytomegalovirus pp65 495–503 group; HBC, HBV core 18–27 wild-type group; HBC-PSI, HBV core 18–27 mutant group; IFN $\gamma$ +, IFN $\gamma$  positive subset; mTGF $\beta$ +, mTGF $\beta$  positive subset; IFN $\gamma$ -/mTGF $\beta$ -, IFN $\gamma$  and mTGF $\beta$  double negative subset. The Friedman test and Dunn's multiple comparisons test were used for comparison of Unstimulated, CMV, and HBC groups and for IFN $\gamma$ +, mTGF $\beta$ +, and IFN $\gamma$ -/mTGF $\beta$ - subsets. The Wilcoxon test was used for comparisons between HBC and HBC-PSI. In (F), the Wilcoxon test was used to compare the HBC and HBC + anti-TGF $\beta$  groups. \* $p < 0.05$ , \*\* $p < 0.01$ , \*\*\*\* $p < 0.0001$ , n.s.: not significant.

The main immune-related signaling pathways identified using this approach are shown in Fig. 2A. Among these three T cell subsets, the IFN $\gamma$ <sup>+</sup> subset exhibited the most diverse gene expression across multiple signaling pathways. In contrast, the mTGF $\beta$ <sup>+</sup> and IFN $\gamma$ <sup>-</sup>/mTGF $\beta$ <sup>-</sup> subsets displayed relatively similar gene expression patterns for many signaling pathways, with the exception of the cytokine-cytokine receptor interaction pathway. GSEA analysis of this pathway further confirmed substantial heterogeneity among the IFN $\gamma$ <sup>+</sup>, mTGF $\beta$ <sup>+</sup>, and IFN $\gamma$ <sup>-</sup>/mTGF $\beta$ <sup>-</sup> subsets (Fig. 2B), supporting the fact that functional divergence underlies their phenotypic classification.

Next, the main genes involved in T cell recognition, activation, differentiation, and the effector stage were analyzed using a heatmap (Fig. 2C), which revealed distinct expression patterns across subsets. The IFN $\gamma$ <sup>+</sup> subset exhibited elevated expression of activation-associated genes (*TNFRSF4*, *TNFRSF9*, *CD28*) and cytokines (*IL2*, *IL4*, *IFN*, *TNF*, *GZMB*). Notably, high expression of *FOXP3* and *PDCD1* in this subset was indicative of an over-activated state rather than exhaustion. This suggests that the IFN $\gamma$ <sup>+</sup> subset is the main effector group among proliferated cells. In contrast, the mTGF $\beta$ <sup>+</sup> subset displayed an inhibitory gene signature characterized by the upregulation of *TIGIT*, *CD244* and *KLRG1*, along with a distinct cytokine profile including *IL6*, *IL15*, and *TGFB1* expression. The IFN $\gamma$ <sup>-</sup>/mTGF $\beta$ <sup>-</sup> subset demonstrated features of functional restraint and exhaustion, including elevated *CD69*, *ENTPD1*, and *CD160* levels. Increased *STAT6* and diminished *TBX21* expression further suggested a transcriptional bias against IFN $\gamma$  production. These results suggested that the IFN $\gamma$ <sup>-</sup>/mTGF $\beta$ <sup>-</sup> subset is hyporeactive. Furthermore, proliferation potential progressively decreased from the IFN $\gamma$ <sup>+</sup> to the IFN $\gamma$ <sup>-</sup>/mTGF $\beta$ <sup>-</sup> subset, as reflected by the declining expression of *MKI67* and *MYC*, consistent with the proliferation data shown in Fig. 1E. The distinct recognition and activation signals associated with these subsets thus appear to elicit the expression of different effector cytokines, leading to different biological functionality.

TCR signaling pathway activation is closely related to downstream gene expression. In the GSEA analysis of the TCR signaling pathway, the top annotated genes *CSF2/IL2/TNF/CTLA4* were highly expressed in the IFN $\gamma$ <sup>+</sup> subset (Fig. 2B), and a similar trend was evident for the transcription factors *IRF4* and *JUN* in the context of T cell metabolism (Fig. 2D). Notably, *IRF4* expression has been reported to correlate directly with TCR-pMHC affinity [12–15]. *CSF2/TNF* expression in the mTGF $\beta$ <sup>+</sup> subset was higher than in the IFN $\gamma$ <sup>-</sup>/mTGF $\beta$ <sup>-</sup> subset, but not with other T cell metabolism related genes. Strikingly, *ZAP70* and *LAT* expression profiles did not match our initial expectations, likely as TCR signaling pathway activation depends on the phosphorylation of the corresponding proteins (*ZAP70* Y319; *LAT* at multiple tyrosine residues), rather than any transcriptional changes. Together, these results

indicated that differential TCR activation drives divergent functional programs across T cell subsets, ultimately shaping their effector, inhibitory, or hyporeactive phenotypes.

### 3.3 pMHC-TCR Affinity May Be a Key Determinant of the Differentiation of Specific CD8<sup>+</sup> T Cell Subsets

T cells recognizing a single epitope exhibit a variety of different TCR sequences. Recognition and matching of different TCRs with the corresponding pMHC complex is critical for CD8<sup>+</sup> T cell function. We thus speculated that pMHC-TCR binding is associated with differential patterns of gene expression. In our analysis, different MFI values were observed when staining HBV-specific CD8<sup>+</sup> T cells with the Tet-HBC tetramer (Supplementary Fig. 2B), consistent with previous studies [9,16], suggesting that these MFI differences may be attributable to TCR-pMHC affinity variance. Further analysis of the frequency and intensity of tetramer staining for each subset of peptide-specific CD8<sup>+</sup> T cells revealed that the IFN $\gamma$ <sup>+</sup> subset exhibited the highest Tet-HBC<sup>+</sup>% and MFI value for tetramer staining, followed by the mTGF $\beta$ <sup>+</sup> subset, while the IFN $\gamma$ <sup>-</sup>/mTGF $\beta$ <sup>-</sup> subset exhibited the lowest intensity (Fig. 3A).

To test whether pMHC-TCR differs among these three subsets, single-cell TCR sequencing was performed. As the TCR-CDR3 region plays an important role in pMHC recognition [17], TRAV/TRBV usage, TRAJ/TRBJ usage, amino acid length, and amino acid sequence of TRAV-CDR3/TRBV-CDR3 for dominant clones among the IFN $\gamma$ <sup>+</sup>, mTGF $\beta$ <sup>+</sup>, and IFN $\gamma$ <sup>-</sup>/mTGF $\beta$ <sup>-</sup> subsets were tested (Fig. 3B and Supplementary Table 2). Clear dominant clones were evident for the IFN $\gamma$ <sup>+</sup> subset. TRAV/TRBV usage and the corresponding CDR3 amino acid sequence for the most dominant clone were TRAV4\*01/TRBV27\*01 and LVGLGGTGTASKLT/ASASLREGLGELF. Greater variability in TRAV/TRBV and TRAJ/TRBJ usage was evident in the mTGF $\beta$ <sup>+</sup> and IFN $\gamma$ <sup>-</sup>/mTGF $\beta$ <sup>-</sup> subsets. The number of amino acids in the CDR3 $\alpha$  region has previously been shown to affect pMHC-TCR affinity [18]. The number of most dominant clones in the IFN $\gamma$ <sup>+</sup>, mTGF $\beta$ <sup>+</sup>, and IFN $\gamma$ <sup>-</sup>/mTGF $\beta$ <sup>-</sup> subsets were 14, 12, and 8, respectively. These data suggested a high level of HBV-specific CD8<sup>+</sup> T cell reactivity in the IFN $\gamma$ <sup>+</sup> subset. Compared with the non-proliferated cells (Healthy control group, HC; data download from a prior study [19]), the TCR Shannon index of the proliferated cells was decreased (Fig. 3C), suggesting that these proliferated cells were peptide-specific.

The ERGO-II model was next applied to characterize TCR-pMHC affinity between different groups. The results of this predictive analysis revealed that the IFN $\gamma$ <sup>+</sup> subset had the highest average score of 0.62785, followed by the mTGF $\beta$ <sup>+</sup> (0.59637) and IFN $\gamma$ <sup>-</sup>/mTGF $\beta$ <sup>-</sup> (0.54319) subsets (Fig. 3D and Supplementary Table 2). These results suggested that the effector subset exhibited the highest TCR-pMHC affinity, followed by the inhibitory subset, whereas the hyporeactive subset had the lowest affinity.

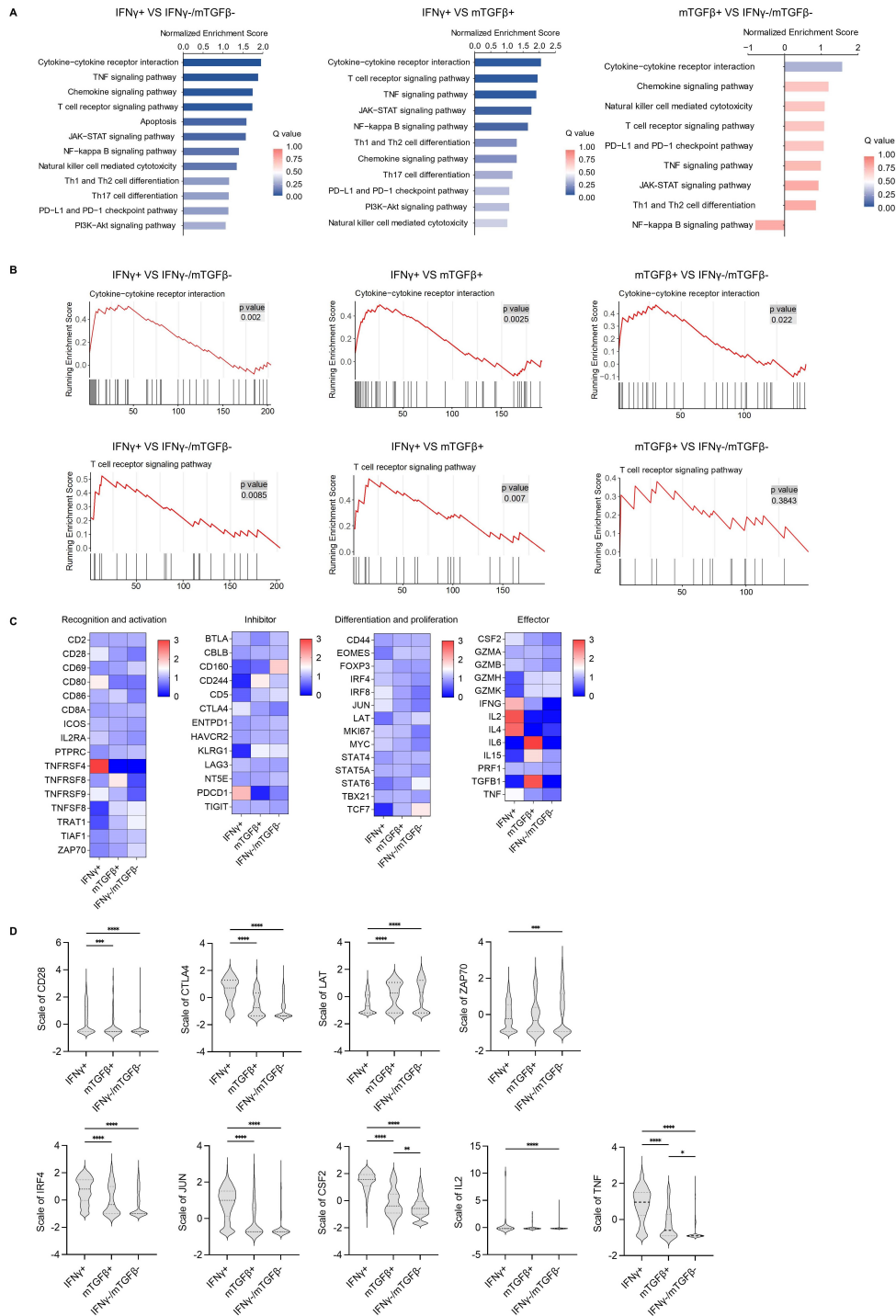


**Fig. 2. Single-cell sequencing analysis of different functional subsets of HBC-specific CD8<sup>+</sup> T cells.** (A) The main immune-related signaling pathways enriched in differentially regulated genes as detected by KEGG enrichment analysis among the IFN $\gamma$ <sup>+</sup>, mTGF $\beta$ <sup>+</sup>, and IFN $\gamma$ <sup>-</sup>/mTGF $\beta$ <sup>-</sup> subsets. (B) GSEA annotation of the IFN $\gamma$ <sup>+</sup>, mTGF $\beta$ <sup>+</sup>, and IFN $\gamma$ <sup>-</sup>/mTGF $\beta$ <sup>-</sup> subsets. Genes in the Cytokine-cytokine receptor interaction pathway (hsa04060) and the T cell receptor signaling pathway (hsa04660) were enriched. (C) Heatmap of the main genes involved in immune-related signaling pathways among the IFN $\gamma$ <sup>+</sup>, mTGF $\beta$ <sup>+</sup>, and IFN $\gamma$ <sup>-</sup>/mTGF $\beta$ <sup>-</sup> subsets. For Z-score colors, red and blue respectively correspond to genes with relatively high and low expression levels. (D) Violin plot of the main genes associated with pMHC-TCR affinity among the IFN $\gamma$ <sup>+</sup>, mTGF $\beta$ <sup>+</sup>, and IFN $\gamma$ <sup>-</sup>/mTGF $\beta$ <sup>-</sup> subsets. IFN $\gamma$ <sup>+</sup>, IFN $\gamma$  positive subset; mTGF $\beta$ <sup>+</sup>, mTGF $\beta$  positive subset; IFN $\gamma$ <sup>-</sup>/mTGF $\beta$ <sup>-</sup>, IFN $\gamma$  and mTGF $\beta$  double negative subset. Q-value < 0.25 was considered statistically significant for the KEGG enrichment analysis.  $p < 0.05$  was considered statistically significant during GSEA annotation. One-way ANOVAs and Tukey's multiple comparisons test were used in (D). \* $p < 0.05$ , \*\* $p < 0.01$ , \*\*\* $p < 0.001$ , \*\*\*\* $p < 0.0001$ .

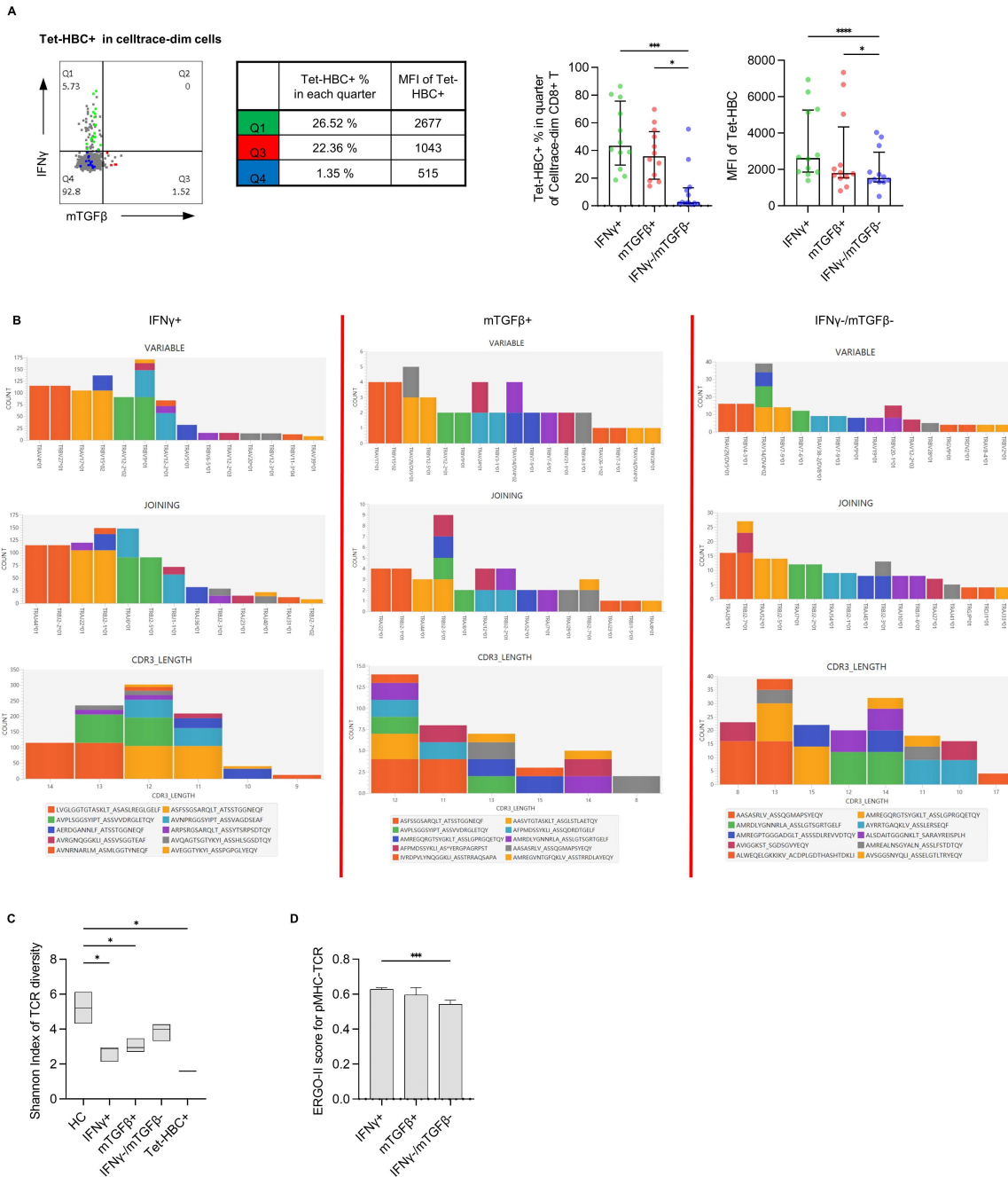


**Fig. 3. Evaluation of pMHC-TCR affinity using the Tet-HBC tetramer and the ERGO-II model.** (A) Left panel: Representative plot from one patient with different Tet-HBC+ % and MFI values in the IFN $\gamma$ + (Q1), mTGF $\beta$ + (Q3), and IFN $\gamma$ -/mTGF $\beta$ - (Q4) groups, with the Tet-HBC+ spots being colored, while the Tet-HBC- spots are shown in gray. Right panel: Bar chart of Tet-HBC+ % and Tet-HBC MFI values among the IFN $\gamma$ +, mTGF $\beta$ +, and IFN $\gamma$ -/mTGF $\beta$ - subsets (n = 12). (B) TCR diversity analysis based on single-cell sequencing of the immune repertoire. Upper panel: TRAV/TRBV (Variable fragment) counts. Middle panel: TRAJ/TRBJ (Joining fragment) counts. Bottom panel: CDR3 amino acid length quantification. Each different colored column represents a single CDR3 sequence. TRAV and TRBV with the same color are paired. (C) Shannon Index for TCR diversity in different groups as analyzed via single-cell sequencing. (D) Affinity predictions made with the ERGO-II model. HC, Healthy control group with non-proliferated T cells; IFN $\gamma$ +, IFN $\gamma$  positive subset; mTGF $\beta$ +, mTGF $\beta$  positive subset; IFN $\gamma$ -/mTGF $\beta$ -, IFN $\gamma$  and mTGF $\beta$  double negative subset; Tet-HBC, HLA-A2 tetramer with the HBV core 18–27 peptide. The Friedman test and Dunn's multiple comparisons test were used in (A). One-way ANOVAs and Tukey's multiple comparisons test were used in (C,D). \* $p < 0.05$ , \*\*\* $p < 0.001$ , \*\*\*\* $p < 0.0001$ .

The individual T cell pool thus appears to differentiate into effector, inhibitory, and hyporeactive subsets according to the degree of TCR-pMHC affinity when responding to a single pMHC.

### 3.4 The $IFN\gamma^+/mTGF\beta^+$ Ratio of HBV-Specific CD8+ T Cells Correlates With Clinical Outcomes

To evaluate the relationship between effector/inhibitory subsets and clinical disease,  $IFN\gamma$  and  $mTGF\beta$  expression in peptide-specific CD8+ T cells was investigated by flow cytometry after *in vitro* expansion and re-stimulation, and the  $IFN\gamma^+/mTGF\beta^+$  ratio was used to assess the response of HBV-specific CD8+ T cells to the virus. Patients in group R achieved the natural functional clearance of HBV, while the CHB patients in the IC and IT groups exhibited impaired HBV clearance, with the IT group showing the lowest clearance capacity. As shown in Fig. 4A, there was a significant difference in the ratio of effector/inhibitory ( $IFN\gamma^+/mTGF\beta^+$ ) subsets among the three groups. The R group displayed the highest value for this ratio, followed by the IC group, while the IT group exhibited the lowest ratio. This variation in the  $IFN\gamma^+/mTGF\beta^+$  ratio was due to differences in the  $IFN\gamma^+$  subset; as the  $mTGF\beta^+$  subset remained relatively consistent across groups (Fig. 4B). To confirm that  $IFN\gamma^+$  frequency is the decisive factor in this analysis, we also examined CMV-specific CD8+ T cells from these same patients. As the patients with CHB showed normal levels of CMV clearance, CMV-specific CD8+ T cells were used as a positive control. Interestingly, in the CMV group, along with the increase in  $IFN\gamma^+$  subset, a corresponding increase in the  $mTGF\beta^+$  subset was also observed (Fig. 4C). Although the size of the  $IFN\gamma^+$  subset was significantly larger in the CMV group as compared to the HBC group, the  $IFN\gamma^+/mTGF\beta^+$  ratio was comparable between the two groups (Fig. 4D). This  $IFN\gamma^+/mTGF\beta^+$  ratio thus appears to be a more sensitive indicator of effector/inhibitory CD8+ T cell subsets as compared to the frequency of  $IFN\gamma^+$  cells with respect to viral clearance among both HBV- and CMV peptide-specific CD8+ T cells.

Consistently, the  $IFN\gamma^+/mTGF\beta^+$  ratio of HBV-DNA-negative samples (ND group) was significantly higher than that of samples with an HBV-DNA load  $>20,000$  IU/mL (Fig. 4E). A similar trend was observed with respect to HBsAg levels, as samples with HBsAg levels  $<200$  ng/mL exhibited a significantly higher  $IFN\gamma^+/mTGF\beta^+$  ratio than those with an HBsAg level  $>10,000$  ng/mL. These results suggested that the  $IFN\gamma^+/mTGF\beta^+$  ratio of effector/inhibitory subsets in HBV-specific CD8+ T cells is a key factor affecting the capacity for viral clearance.

## 4. Discussion

Some controversy persists regarding the definition of specific CD8+ T cells. Previous studies have reported a correlation between total T cells and HBV-specific CD8+ T cells in terms of phenotypic and functional characteristics, with total T cells also reflecting the clinical severity of HBV infection [20]. These findings suggest that some specific CD8+ T cells may not yet have been fully characterized. In our study, Tet-HBC+ T cell subsets were detected among proliferated T cells from 21 out of 60 individuals, including 6/16 in the IT group, 11/30 in the IC group, and 4/14 in the R group. Based on previous studies [21,22], we propose that genetic factors such as HLAA2 polymorphisms, rather than disease status, contribute to the limited detection efficiency of specific CD8+ T cells using a tetramer-based approach. Moreover, a substantial proportion of HBV-specific CD8+ T cells in the IT group exhibited low affinity and diminished immune function, which further limits their detection via conventional tetramer staining. In this study, specific CD8+ T cells were defined through *in vitro* expansion following peptide stimulation. Although expanded cells show some changes in their phenotype and functionality [23], this approach enabled the detection of a broader spectrum of functional phenotypes, particularly for inhibitory subsets of T cells that are often overlooked in the context of tetramer staining. This provides a valuable complementary strategy for the comprehensive profiling of specific CD8+ T cells, as well as a supplemental strategy that can improve results obtained through tetramer detection.

The HBV core 18–27 epitope is a classical target of HLA-A\*0201-restricted CD8+ T-cell responses in HBV infection. However, in Asian populations, HBV genotypes B and C almost exclusively carry this V27I mutation (FLPS-DFFPSI) [21], which impairs peptide binding to HLA-A\*0201 [24]. Despite this reduced affinity, our data confirmed that both wild-type and variant peptides induce T-cell proliferation and could be detected by HBV core 18–27 Tetramer (Supplementary Fig. 2A), and V27-primed T cells cross-recognize the I27 variant (Supplementary Fig. 3A). These findings are consistent with previous studies demonstrating cross-reactivity between V27 and I27 epitopes [25], suggesting that TCR affinity, rather than MHC binding, dominates the functional response.

Hyporeactive T cells have been conventionally classified into three categories: exhausted T cells exhibiting CD45RO+/CD57+/CD95+/PD-1+/CTLA-4+/Tim-3+/LAG-3+/BTLA+ expression; anergic T cells expressing LAG-3+/PD-1+; and senescent T cells expressing KLRG1+/CD28-/CD57+ [8]. These cells generally exhibit limited proliferative capacity [26]. Although *in vitro* expansion may partially select against such hypoproliferative cells, some reactive subsets with a distinct expression pattern could nonetheless be detected (Supplementary Fig. 4). In this study, by leveraging the natural model of CHB infection, HBV-specific CD8+ T

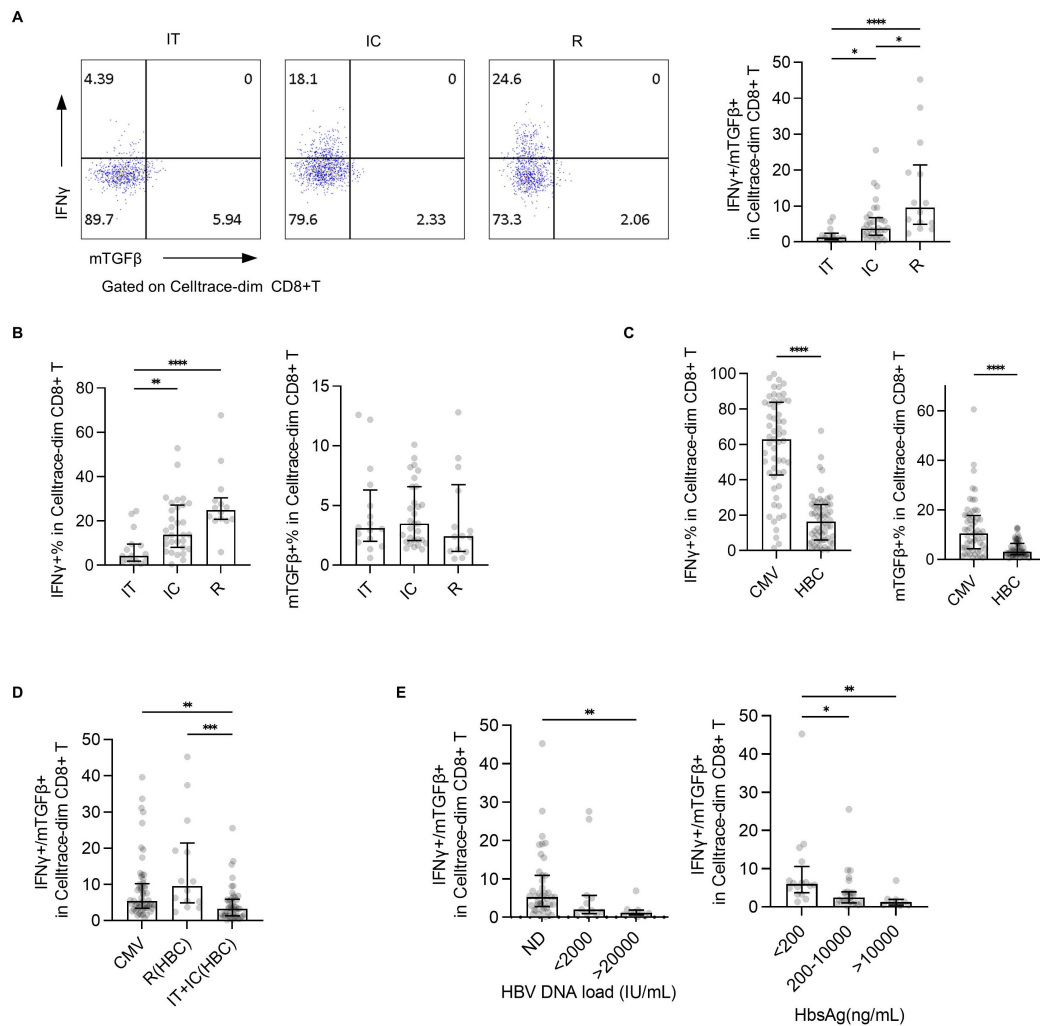


**Fig. 4. Evaluation of the IFN $\gamma$ +/mTGF $\beta$ + ratio of peptide-specific CD8+ T cells in patients with different disease outcomes.** (A) The IFN $\gamma$ +/mTGF $\beta$ + ratios for the IT, IC, and R groups as assessed by flow cytometry. Left panel: representative plot. Right panel: bar chart with the IT, IC, and R groups. (B) IFN $\gamma$  and mTGF $\beta$  expression on IT, IC, and R group. (C) IFN $\gamma$  and mTGF $\beta$  expression in the CMV and HBC groups. (D) IFN $\gamma$ +/mTGF $\beta$ + ratios for the CMV, HBC-R, and HBC-CHB groups. (E) Correlation between the IFN $\gamma$ +/mTGF $\beta$ + ratio and both HBV DNA load and HbsAg levels. CMV, Cytomegalovirus pp65 495–503 group; HBC, HBV core 18–27 group; IT, immune tolerance stage; IC, inactive carrier stage; R, acute resolved patients; CHB, chronic hepatitis B patients. ND: negative for HBV DNA detection. The Kruskal-Wallis test and Dunn’s multiple comparisons test were used in (A,B,D,E), while the Wilcoxon test was used in (C). \* $p < 0.05$ , \*\* $p < 0.01$ , \*\*\* $p < 0.001$ , \*\*\*\* $p < 0.0001$ .

cells were classified into three subsets: an effector subset (IFN $\gamma$ +), an inhibitory subset (mTGF $\beta$ +), and a hyporeactive subset (IFN $\gamma$ -/mTGF $\beta$ -), each demonstrating unique transcriptional and functional profiles.

In this study, the effector subset exhibited elevated expression of annotated genes associated with the cytokine-cytokine receptor interaction pathway, consistent with the functional capacity of these cells. Notably, both *PDCD1* and *FOXP3* were highly expressed in the effector subset, whereas they were expressed at lower levels in the hyporeactive and inhibitory subsets, suggesting that in the context of HBV-specific CD8+ T cells, these markers may not primarily serve as indicators of inhibition, consistent with

the recent results from Luo *et al.* [27]. The hyporeactive IFN $\gamma$ -/mTGF $\beta$ - subset, in contrast, displayed elevated expression of *ENTPD1*, *CD69*, and *CD160*, consistent with an altered activation state after stimulation. *CD160* has been shown to inhibit IL-2 secretion through herpes virus entry mediator (HVEM) [28]. Concurrently, this subset also presented with the upregulation of *STAT6*, which has been reported to affect the differentiation of CD8+ T cells from Stem-like/Progenitor exhausted T cells (Tprog cells) to Terminally differentiated exhausted T cells (Term cells) by antagonizing the TGF $\beta$ -BCL6 and IL-2-BLIMP-1 signaling axis [29]. *TCF7* was exclusively highly expressed in the IFN $\gamma$ -/mTGF $\beta$ - subset of CD8+ T cells. In a pre-

vious study, TCF7 was shown to directly bind and activate the enhancer regions of EOMES, Bcl-2, and Wnt target genes, suppressing exhaustion-related genes (*PDCDI*, *TOX*) while promoting the expression of memory-related genes [30].

As most cells within this subset were negative for tetramer detection, they have likely been overlooked in prior tetramer-based studies focused on specific CD8<sup>+</sup> T cells. Collectively, these results suggest that the IFN $\gamma$ -/mTGF $\beta$ - subset identified here represents a unique population distinct from the conventionally defined exhausted subpopulation, exhibiting properties of both hyporesponsiveness and memory potential. In addition, the ratio of the IFN $\gamma$ -/mTGF $\beta$ - subset was correlated with HBV viral load in our study, suggesting that there may be other regulatory mechanisms that influence the behavior of this hyporeactive subset and warrant further investigation.

TGF $\beta$  is an important immunomodulatory molecule involved in maintaining immune tolerance, promoting Th17 cell differentiation, and regulating immune homeostasis [31]. Membrane-bound TGF $\beta$  exhibits similar biological activity [32]. It is presented on the cell surface in the form of a latent related peptide (LAP)-TGF $\beta$  complex by binding to latent TGF $\beta$  binding protein (LTBP). It exerts its biological functions via matrix metalloproteinase (MMP) cleavage, integrin-mediated mechanical activation, exposure to an acidic environment or reactive oxygen species, and intercellular contact. Consistent with our previous studies [10], neutralization of TGF- $\beta$  signaling using a specific antibody led to a significant increase in IFN $\gamma$  production in the present study. It has been reported that TGF $\beta$  can upregulate IL-6, activate STAT3, in addition to upregulating VEGF and IL-10, thereby suppressing anti-tumor activity [33]. We also found that the upregulation of the gene encoding TGF $\beta$  was accompanied by the upregulation of *IL6*. Given its potent immunosuppressive activity and frequent co-expression with other inhibitory molecules [34], mTGF $\beta$  was used as a surface marker in this study to identify the inhibitory subset of CD8<sup>+</sup> T cells. Although the upstream regulators of mTGF $\beta$  expression remain incompletely defined, its functional significance supports its utility as a reliable phenotypic marker for an inhibitory subset of cells.

The post-proliferation frequency of specific CD8<sup>+</sup> T cells is related to their precursor frequency, as the proliferative capacity (amplification index) remains consistent across different epitopes [35]. In this study, the post-proliferation frequency of HBV core-specific CD8<sup>+</sup> T cells did not correlate with the clinical outcome of hepatitis B infection. The variation in precursor frequency of specific CD8<sup>+</sup> T cells among individuals is likely attributable to inherent differences in their T cell repertoire. Age has been identified as a contributing factor associated with the precursor frequency of IFN $\gamma$ + peptide-specific CD8<sup>+</sup> T cells relative to HBsAg concentration, with a significant de-

crease in the frequency of HBV env-specific CD8<sup>+</sup> T cells after 30 years of age [36].

Studies have also shown that specific T cells responsive to different antigenic epitopes have different reactivity [5]. Recent evidence has further indicated that antigen types influence the aging trajectory of memory T cells [37]. Our findings extend this concept by demonstrating that even among specific T cells responsive to a single epitope, considerable functional heterogeneity exists. Notably, we observed no differences in the proliferation or function of specific CD8<sup>+</sup> T cells between the HBC and HBC-PSI groups, suggesting that this particular viral mutation does not substantially alter the phenotype of specific CD8<sup>+</sup> T cells, which is consistent with the findings of Hoogveen *et al.* [6]. We hypothesize that it is the T cell repertoire in different individuals, rather than any viral mutation, that determines the clinical outcome of HBV infection. However, when combined with different HLA alleles, this mutation will also lead to the impairment of T cell reactivity [38]. This factor should be carefully considered in the application of T cell therapy.

The recognition of the TCRs of specific CD8<sup>+</sup> T cells is not merely specific to a peptide, but to an intact pMHC complex [17,39]. This affinity between pMHC complex and TCR serves as a critical indicator of the strength of immune responses against a given antigen, and is influenced collectively by antigen epitopes, MHC type, TCR sequence and expression levels, costimulatory molecules, and the TCR signaling pathway [40,41]. Recent studies have analyzed the phenotypes and functions of T cells associated with different clinical outcomes by single-cell sequencing and found that there are more exhausted CD8<sup>+</sup> T cells in immune-activated and acute convalescent patients [19]. Our single-cell sequencing results focused specifically on proliferating CD8<sup>+</sup> T cells also showed that TCR diversity was significantly reduced in the effector subset (IFN $\gamma$ +) compared to the inhibitory subset (mTGF $\beta$ +) and the hyporeactive subset (IFN $\gamma$ -/mTGF $\beta$ -). A parallel trend was observed in terms of the expression of TCR signaling pathway-related genes. Furthermore, both the tetramer assay and ERGO-II model predictions supported a higher degree of affinity in the effector subset. Notably, higher pMHC-TCR affinity does not invariably correlate with improved functionality. Recent studies have shown that in tetramer-positive cells, TIM3 and TOX, which are indicative of hyporeactivity, were highly expressed in the highest affinity group [42]. Together, these results demonstrate that the TCR-pMHC affinity serves as a key determinant of the function of these three different subgroups of CD8<sup>+</sup> T cells.

Of note, we detected a proportion of TRGV9<sup>+</sup> and TRDV2<sup>+</sup>  $\gamma\delta$  T cells following *in vitro* expansion of specific CD8<sup>+</sup> T cells. This observation is consistent with previous reports that  $\gamma\delta$  T cells can non-specifically proliferate in response to cytokines such as IL2 during *in vitro* culture, even in the absence of specific antigen stimulation [43,44].

This phenomenon is particularly prominent in cultures enriched for innate-like T cells, where  $\gamma\delta$  T cells, including a distinct  $CD8\alpha\beta^+$  subset, exhibit robust proliferation driven by shared signaling pathways [45]. Mechanistically, activated  $\gamma\delta$  T cells can function as antigen-presenting cells ( $\gamma\delta$  TAPCs) and secrete IL4/IL12, thereby directly supporting the expansion and effector differentiation of  $CD8^+ \alpha\beta$  T cells. Thus, the detection of TRGV/TRDV transcripts does not reflect non-specific contamination but rather indicates a physiologically relevant, cytokine-driven co-expansion that may contribute to the overall potency of the cultured T cell product.

Serum conversion of HBeAg is a clinically important prognostic marker in hepatitis B infection. In CHB patients, HBeAg- individuals exhibit enhanced functionality of HBV core-specific  $CD8^+$  T cells as compared to HBeAg+ individuals [6]. Studies employing ELISPOT assays after stimulation with HBV peptide pools have demonstrated that IFN $\gamma$  levels are inversely correlated with HBV DNA and HBsAg concentrations [46]. Some investigators have categorized CHB into HBs<sup>lo</sup> (HBsAg <500 IU/mL) and HBs<sup>hi</sup> (HBsAg >50,000 IU/mL) cases. They further found that the frequency of IFN $\gamma$ +/TNF $\alpha$ + HBs<sup>lo</sup> HBV-specific  $CD8^+$  T cells was 85%, and the frequency of IFN $\gamma$ +/IL-2+  $CD4^+$  T cells was 60%, whereas the corresponding frequency for HBs<sup>hi</sup> cells were only 33% and 13%, respectively [47]. Our findings align with these observations. The IFN $\gamma$ +/mTGF $\beta$ + ratio was used as a functional indicator of the effector and inhibitory subsets of HBV-specific  $CD8^+$  T cells. The IFN $\gamma$ /mTGF $\beta$  ratio of HBV-specific  $CD8^+$  T cells was correlated with the clinical outcome of HBV infection, HBV DNA level, and HBsAg level. We also noted that for the same patients in the R group, the IFN $\gamma$ +/mTGF $\beta$ + ratio varied widely among individuals, and the correlation between HBsAg concentration and the specific T cell IFN $\gamma$ +/mTGF $\beta$ + ratio was unclear. More precise indicators are thus needed for use in this context, with HBcrAg offering promise [48].

Although the TCR-pMHC affinity of specific  $CD8^+$  T cells cannot be altered, it can be modified through immune-focused interventions such as therapeutic vaccines, PD-1 blockade, metabolic interventions, TLR antagonists, TCR-T, CAR-T, or soluble TCRS strategies [15,49–52], offering potential opportunities to redirect T cell clones such that they differentiate into effector subsets. Hypoxic tumor microenvironments have been reported to promote the generation of  $CD39^+$  T cells, and microenvironmental modulation can alter the immunosuppressive status of these exhausted T cells [53]. Similarly, a recombinant fusion protein including IL-10 and the IgG Fc region has been shown to activate the pyruvate/MPC pathway within terminally depleted T cells by reprogramming cellular metabolism, thereby enhancing oxidative phosphorylation levels and the anti-tumor efficacy of these immune cells [54]. *In vitro* metabolic intervention with MitoQ has also been shown

to alter the ratio of effector/inhibitory subsets of specific  $CD8^+$  T cells [55]. Wang *et al.* [10] previously confirmed the efficacy of metabolic interventions by analyzing HBV-specific T cell responses in CHB patients with different disease outcomes, including mitochondria-targeted antioxidants (Mito-TEMPO and MitoQ), polyphenol compounds (resveratrol + oleuropein), and cholesterol acyltransferase inhibitors (AVASIMIBE + K-604), which regulate HBV-specific T cell function in patients with CHB [56]. Notably, these metabolic interventions did not show a substantial influence on HBV core-specific  $CD8^+$  T cells despite significantly enhancing IFN $\gamma$  expression among HBV env-specific  $CD8^+$  T cells. This differential responsiveness underscores the epitope-dependent nature of metabolic modulation in specific  $CD8^+$  T cells.

## 5. Limitations

Several limitations should be acknowledged in the present study. First, this was an observational study lacking any strict control over potential confounding variables, which may have introduced considerable bias. As such, our conclusions require further validation through more rigorous clinical investigation, including prospective studies. Second, HLA-A2 subtypes were not determined for the study participants, highlighting another factor that should be taken into account in future research. Third, although healthy individuals were initially intended as controls, the precursor frequency of HBV-specific T cells was extremely low in this population, making them difficult to detect even after *in vitro* expansion; we therefore used convalescent patients as a surrogate for individuals with a natural immune response, representing another methodological limitation. Finally, the present study sought to demonstrate that CHB infection is mainly driven by intrinsic interindividual differences in the T cell repertoire, rather than by T cell exhaustion. However, the current evidence is not sufficiently robust to support this conclusion, and in future studies, T cells from HBV-naïve children may be used as controls to further verify this hypothesis.

## 6. Conclusions

This study explored the differentiation of T cell subsets and the association of these subsets with TCR-pMHC affinity in the context of CHB infection. Overall, our results support a model in which functionally distinct immune responses can be induced by single peptide-specific  $CD8^+$  T cells. These findings provide a theoretical basis to inform the further development of T cell-based immunotherapies. Future studies should focus on approaches to modulating the balance between effector and inhibitory  $CD8^+$  T cell subsets through *in vitro* interventions, thereby enhancing antiviral immune efficacy.

## Availability of Data and Materials

The original contributions presented in the study are included in the article/Supplementary Material. Further inquiries can be directed to the corresponding authors. The NGS datasets presented in this study can be found in the NCBI SRA BioProject, accession No.: SUB14183699.

## Author Contributions

Conceive and design the experiments: XWW, XFW, SL; perform the experiments: ZS, XW, JZ; collect the clinical samples: ZS, LO; analyze the data: MW, TZ, LO; prepare the manuscript: ZS. All authors contributed to editorial changes in the manuscript. All authors read and approved the final manuscript. All authors have participated sufficiently in the work and agreed to be accountable for all aspects of the work.

## Ethics Approval and Consent to Participate

The study was carried out in accordance with the guidelines of the Declaration of Helsinki. It was approved by the Ethics Committee of Hubei No.3 People's Hospital (Approval No.: BA2025002). All the samples used in the experiment were from discarded samples after clinical examination and applied for exemption from informed consent.

## Acknowledgment

The authors would like to thank director Yuqi Qu in Basic Scientific Research Reagent Department of MBL for kind provision of the expansion protocol of peptide-specific CD8<sup>+</sup> T cells. We also thank Dr. Chen Chen in Department of Breast and Thyroid Surgery of Union Hospital of Huazhong University of Science for her extensive revision of the manuscript.

## Funding

This work was supported by the National Natural Science Foundation, China (81871226, 32170920) and the Research Foundation of the Health Commission of Hubei Province Scientific Research Project, China (WJ2021F134).

## Conflicts of Interest

The authors declare no conflicts of interest.

## Supplementary Material

Supplementary material associated with this article can be found, in the online version, at <https://doi.org/10.31083/FBL51459>.

## References

- [1] Burki T. WHO's 2024 global hepatitis report. *The Lancet. Infectious Diseases*. 2024; 24: e362–e363. [https://doi.org/10.1016/S1473-3099\(24\)00307-4](https://doi.org/10.1016/S1473-3099(24)00307-4).
- [2] You H, Wang F, Li T, Xu X, Sun Y, Nan Y, *et al.* Guidelines for the Prevention and Treatment of Chronic Hepatitis B (version 2022). *Journal of Clinical and Translational Hepatology*. 2023; 11: 1425–1442. <https://doi.org/10.14218/JCTH.2023.00320>.
- [3] Nitschke K, Luxenburger H, Kiraithe MM, Thimme R, Neumann-Haefelin C. CD8<sup>+</sup> T-Cell Responses in Hepatitis B and C: The (HLA-) A, B, and C of Hepatitis B and C. *Digestive Diseases (Basel, Switzerland)*. 2016; 34: 396–409. <https://doi.org/10.1159/000444555>.
- [4] Heim K, Neumann-Haefelin C, Thimme R, Hofmann M. Heterogeneity of HBV-Specific CD8<sup>+</sup> T-Cell Failure: Implications for Immunotherapy. *Frontiers in Immunology*. 2019; 10: 2240. <https://doi.org/10.3389/fimmu.2019.02240>.
- [5] Bertoletti A, Kennedy PTF. HBV antiviral immunity: not all CD8 T cells are born equal. *Gut*. 2019; 68: 770–773. <https://doi.org/10.1136/gutjnl-2018-317959>.
- [6] Hoogeveen RC, Robidoux MP, Schwarz T, Heydmann L, Cheney JA, Kvistad D, *et al.* Phenotype and function of HBV-specific T cells is determined by the targeted epitope in addition to the stage of infection. *Gut*. 2019; 68: 893–904. <https://doi.org/10.1136/gutjnl-2018-316644>.
- [7] Bertoletti A, Ferrari C. Adaptive immunity in HBV infection. *Journal of Hepatology*. 2016; 64: S71–S83. <https://doi.org/10.1016/j.jhep.2016.01.026>.
- [8] Davoodzadeh Gholami M, Kardar GA, Saeedi Y, Heydari S, Garssen J, Falak R. Exhaustion of T lymphocytes in the tumor microenvironment: Significance and effective mechanisms. *Cellular Immunology*. 2017; 322: 1–14. <https://doi.org/10.1016/j.cellimm.2017.10.002>.
- [9] Alanio C, Lemaitre F, Law HKW, Hasan M, Albert ML. Enumeration of human antigen-specific naive CD8<sup>+</sup> T cells reveals conserved precursor frequencies. *Blood*. 2010; 115: 3718–3725. <https://doi.org/10.1182/blood-2009-10-251124>.
- [10] Wang Z, Ouyang L, Liang Z, Chen J, Yu Q, Jeza VT, *et al.* CD8(low)CD28(-) T Cells: A Human CD8 T-Suppressor Subpopulation With Alloantigen Specificity Induced by Soluble HLA-A2 Dimer In Vitro. *Cell Transplantation*. 2015; 24: 2129–2142. <https://doi.org/10.3727/096368914X683575>.
- [11] Springer I, Tickotsky N, Louzoun Y. Contribution of T Cell Receptor Alpha and Beta CDR3, MHC Typing, V and J Genes to Peptide Binding Prediction. *Frontiers in Immunology*. 2021; 12: 664514. <https://doi.org/10.3389/fimmu.2021.664514>.
- [12] Yao S, Buzo BF, Pham D, Jiang L, Taparowsky EJ, Kaplan MH, *et al.* Interferon regulatory factor 4 sustains CD8(+) T cell expansion and effector differentiation. *Immunity*. 2013; 39: 833–845. <https://doi.org/10.1016/j.immuni.2013.10.007>.
- [13] Man K, Miasari M, Shi W, Xin A, Henstridge DC, Preston S, *et al.* The transcription factor IRF4 is essential for TCR affinity-mediated metabolic programming and clonal expansion of T cells. *Nature Immunology*. 2013; 14: 1155–1165. <https://doi.org/10.1038/ni.2710>.
- [14] Tsui C, Heyden L, Wen L, Gago da Graça C, Potemkin N, Frolov A, *et al.* Lymph nodes fuel KLF2-dependent effector CD8<sup>+</sup> T cell differentiation during chronic infection and checkpoint blockade. *Nature Immunology*. 2025; 26: 1752–1765. <https://doi.org/10.1038/s41590-025-02276-7>.
- [15] Park BV, Pan F. Metabolic regulation of T cell differentiation and function. *Molecular Immunology*. 2015; 68: 497–506. <https://doi.org/10.1016/j.molimm.2015.07.027>.
- [16] Wieland D, Kemming J, Schuch A, Emmerich F, Knolle P, Neumann-Haefelin C, *et al.* TCF1<sup>+</sup> hepatitis C virus-specific CD8<sup>+</sup> T cells are maintained after cessation of chronic antigen stimulation. *Nature Communications*. 2017; 8: 15050. <https://doi.org/10.1038/ncomms15050>.
- [17] Miles JJ, McCluskey J, Rossjohn J, Gras S. Understanding the complexity and malleability of T-cell recognition. *Immunology*

- and Cell Biology. 2015; 93: 433–441. <https://doi.org/10.1038/icb.2014.112>.
- [18] Chen G, Yang X, Ko A, Sun X, Gao M, Zhang Y, *et al.* Sequence and Structural Analyses Reveal Distinct and Highly Diverse Human CD8<sup>+</sup> TCR Repertoires to Immunodominant Viral Antigens. *Cell Reports*. 2017; 19: 569–583. <https://doi.org/10.1016/j.celrep.2017.03.072>.
- [19] Zhang C, Li J, Cheng Y, Meng F, Song JW, Fan X, *et al.* Single-cell RNA sequencing reveals intrahepatic and peripheral immune characteristics related to disease phases in HBV-infected patients. *Gut*. 2023; 72: 153–167. <https://doi.org/10.1136/gutjnl-2021-325915>.
- [20] Rossi M, Vecchi A, Tiezzi C, Barili V, Fiscaro P, Penna A, *et al.* Phenotypic CD8 T cell profiling in chronic hepatitis B to predict HBV-specific CD8 T cell susceptibility to functional restoration in vitro. *Gut*. 2023; 72: 2123–2137. <https://doi.org/10.1136/gutjnl-2022-327202>.
- [21] Tan AT, Loggi E, Boni C, Chia A, Gehring AJ, Sastry KSR, *et al.* Host ethnicity and virus genotype shape the hepatitis B virus-specific T-cell repertoire. *Journal of Virology*. 2008; 82: 10986–10997. <https://doi.org/10.1128/JVI.01124-08>.
- [22] Bertoletti A, Southwood S, Chesnut R, Sette A, Falco M, Ferrara GB, *et al.* Molecular features of the hepatitis B virus nucleocapsid T-cell epitope 18–27: interaction with HLA and T-cell receptor. *Hepatology* (Baltimore, Md.). 1997; 26: 1027–1034. <https://doi.org/10.1002/hep.510260435>.
- [23] Bertoletti A. The challenges of adopting immunological biomarkers in the management of chronic HBV infection. *Journal of Hepatology*. 2022; 77: 299–301. <https://doi.org/10.1016/j.jhep.2022.03.028>.
- [24] Bertoletti A, Costanzo A, Chisari FV, Levrero M, Artini M, Sette A, *et al.* Cytotoxic T lymphocyte response to a wild type hepatitis B virus epitope in patients chronically infected by variant viruses carrying substitutions within the epitope. *The Journal of Experimental Medicine*. 1994; 180: 933–943. <https://doi.org/10.1084/jem.180.3.933>.
- [25] Liu HG, Chen WW, Fan ZP, Yang HY, Shi M, Zhang Z, *et al.* The high prevalence of the I27 mutant HBcAg18–27 epitope in Chinese HBV-infected patients and its cross-reactivity with the V27 prototype epitope. *Clinical Immunology* (Orlando, Fla.). 2007; 125: 337–345. <https://doi.org/10.1016/j.clim.2007.06.010>.
- [26] Singer M, Elsayed AM, Husseiny MI. Regulatory T-cells: The Face-off of the Immune Balance. *Frontiers in Bioscience* (Landmark Edition). 2024; 29: 377. <https://doi.org/10.31083/j.fb12911377>.
- [27] Luo S, Larson JH, Blazar BR, Abdi R, Bromberg JS. Foxp3<sup>+</sup>CD8<sup>+</sup> regulatory T cells: bona fide Tregs with cytotoxic function. *Trends in Immunology*. 2025; 46: 324–337. <https://doi.org/10.1016/j.it.2025.02.010>.
- [28] Kim TJ, Park G, Kim J, Lim SA, Kim J, Im K, *et al.* CD160 serves as a negative regulator of NKT cells in acute hepatic injury. *Nature Communications*. 2019; 10: 3258. <https://doi.org/10.1038/s41467-019-10320-y>.
- [29] Sun Q, Cai D, Liu D, Zhao X, Li R, Xu W, *et al.* BCL6 promotes a stem-like CD8<sup>+</sup> T cell program in cancer via antagonizing BLIMP1. *Science Immunology*. 2023; 8: eadh1306. <https://doi.org/10.1126/sciimmunol.adh1306>.
- [30] Zhu Y, Wang W, Wang X. Roles of transcriptional factor 7 in production of inflammatory factors for lung diseases. *Journal of Translational Medicine*. 2015; 13: 273. <https://doi.org/10.1186/s12967-015-0617-7>.
- [31] Batlle E, Massagué J. Transforming Growth Factor- $\beta$  Signaling in Immunity and Cancer. *Immunity*. 2019; 50: 924–940. <https://doi.org/10.1016/j.immuni.2019.03.024>.
- [32] Ahn YO, Lee JC, Sung MW, Heo DS. Presence of membrane-bound TGF-beta1 and its regulation by IL-2-activated immune cell-derived IFN-gamma in head and neck squamous cell carcinoma cell lines. *Journal of Immunology* (Baltimore, Md.: 1950). 2009; 182: 6114–6120. <https://doi.org/10.4049/jimmunol.0803725>.
- [33] Yu H, Kortylewski M, Pardoll D. Crosstalk between cancer and immune cells: role of STAT3 in the tumour microenvironment. *Nature Reviews. Immunology*. 2007; 7: 41–51. <https://doi.org/10.1038/nri1995>.
- [34] Ouyang L, Li X, Liang Z, Yang D, Gong F, Shen G, *et al.* CD8low T-cell subpopulation is increased in patients with chronic hepatitis B virus infection. *Molecular Immunology*. 2013; 56: 698–704. <https://doi.org/10.1016/j.molimm.2013.07.003>.
- [35] Schulien I, Kemming J, Oberhardt V, Wild K, Seidel LM, Killmer S, *et al.* Characterization of pre-existing and induced SARS-CoV-2-specific CD8<sup>+</sup> T cells. *Nature Medicine*. 2021; 27: 78–85. <https://doi.org/10.1038/s41591-020-01143-2>.
- [36] Le Bert N, Gill US, Hong M, Kunasegaran K, Tan DZM, Ahmad R, *et al.* Effects of Hepatitis B Surface Antigen on Virus-Specific and Global T Cells in Patients With Chronic Hepatitis B Virus infection. *Gastroenterology*. 2020; 159: 652–664. <https://doi.org/10.1053/j.gastro.2020.04.019>.
- [37] Sturmlechner I, Jain A, Hu B, Jadhav RR, Cao W, Okuyama H, *et al.* Antigen specificity shapes distinct aging trajectories of memory CD8<sup>+</sup> T cells. *Nature Communications*. 2025; 16: 6394. <https://doi.org/10.1038/s41467-025-61627-y>.
- [38] Walker A, Schwarz T, Brinkmann-Paulukat J, Wisskirchen K, Menne C, Alizei ES, *et al.* Immune escape pathways from the HBV core<sub>18–27</sub> CD8 T cell response are driven by individual HLA class I alleles. *Frontiers in Immunology*. 2022; 13: 1045498. <https://doi.org/10.3389/fimmu.2022.1045498>.
- [39] Chen DG, Xie J, Su Y, Heath JR. T cell receptor sequences are the dominant factor contributing to the phenotype of CD8<sup>+</sup> T cells with specificities against immunogenic viral antigens. *Cell Reports*. 2023; 42: 113279. <https://doi.org/10.1016/j.celrep.2023.113279>.
- [40] Campillo-Davo D, Flumens D, Lion E. The Quest for the Best: How TCR Affinity, Avidity, and Functional Avidity Affect TCR-Engineered T-Cell Antitumor Responses. *Cells*. 2020; 9: 1720. <https://doi.org/10.3390/cells9071720>.
- [41] Wu LZ, Balyan R, Brzostek J, Zhao X, Gascoigne NRJ. Time required for commitment to T cell proliferation depends on TCR affinity and cytokine response. *EMBO Reports*. 2023; 24: e54969. <https://doi.org/10.15252/embr.202254969>.
- [42] Singhaviranon S, Dempsey JP, Hagymasi AT, Mandoiu II, Srivastava PK. Low-avidity T cells drive endogenous tumor immunity in mice and humans. *Nature Immunology*. 2025; 26: 240–251. <https://doi.org/10.1038/s41590-024-02044-z>.
- [43] Kjeldsen-Kragh J, Quayle AJ, Skålhegg BS, Sioud M, Førre O. Selective activation of resting human gamma delta T lymphocytes by interleukin-2. *European Journal of Immunology*. 1993; 23: 2092–2099. <https://doi.org/10.1002/eji.1830230908>.
- [44] Sumaria N, Fiala GJ, Inácio D, Curado-Avelar M, Cachucho A, Pinheiro R, *et al.* Perinatal thymic-derived CD8 $\alpha\beta$ -expressing  $\gamma\delta$  T cells are innate IFN- $\gamma$  producers that expand in IL-7R-STAT5B-driven neoplasms. *Nature Immunology*. 2024; 25: 1207–1217. <https://doi.org/10.1038/s41590-024-01855-4>.
- [45] Le S, Dooley N, Murphy D, Liu S, Gandolfo LC, Ge Z, *et al.*  $\gamma\delta$  T cell-derived IL-4 initiates CD8<sup>+</sup> T cell immunity. *Nature Immunology*. 2026; 27: 295–307. <https://doi.org/10.1038/s41590-025-02397-z>.
- [46] Loggi E, Bihl FK, Cursaro C, Granieri C, Galli S, Brodosi L, *et al.* Virus-specific immune response in HBeAg-negative chronic hepatitis B: relationship with clinical profile and HBeAg serum levels. *PLoS One*. 2013; 8: e65327. <https://doi.org/10.1371/jour>

nal.pone.0065327.

- [47] Kim JH, Ghosh A, Ayithan N, Romani S, Khanam A, Park JJ, *et al.* Circulating serum HBsAg level is a biomarker for HBV-specific T and B cell responses in chronic hepatitis B patients. *Scientific Reports*. 2020; 10: 1835. <https://doi.org/10.1038/s41598-020-58870-2>.
- [48] Aliabadi E, Urbanek-Quaing M, Maasoumy B, Bremer B, Grasshoff M, Li Y, *et al.* Impact of HBsAg and HBcrAg levels on phenotype and function of HBV-specific T cells in patients with chronic hepatitis B virus infection. *Gut*. 2022; 71: 2300–2312. <https://doi.org/10.1136/gutjnl-2021-324646>.
- [49] Maini MK, Burton AR. Restoring, releasing or replacing adaptive immunity in chronic hepatitis B. *Nature Reviews. Gastroenterology & Hepatology*. 2019; 16: 662–675. <https://doi.org/10.1038/s41575-019-0196-9>.
- [50] Allahmoradi E, Mohammadi R, Kheirandish Zarandi P, Alavian SM, Heiat M. The CD8+ T cell exhaustion mechanisms in chronic hepatitis B infection and immunotherapeutic strategies: a systematic review. *Expert Review of Clinical Immunology*. 2023; 19: 671–688. <https://doi.org/10.1080/1744666X.2023.2198209>.
- [51] Fergusson JR, Wallace Z, Connolly MM, Woon AP, Suckling RJ, Hine DW, *et al.* Immune-Mobilizing Monoclonal T Cell Receptors Mediate Specific and Rapid Elimination of Hepatitis B-Infected Cells. *Hepatology (Baltimore, Md.)*. 2020; 72: 1528–1540. <https://doi.org/10.1002/hep.31503>.
- [52] Garcia Castillo J, DeBarge R, Mende A, TenVooren I, Marquez DM, Straub A, *et al.* A mass cytometry method pairing T cell receptor and differentiation state analysis. *Nature Immunology*. 2024; 25: 1754–1763. <https://doi.org/10.1038/s41590-024-01937-3>.
- [53] Vignali PDA, DePeaux K, Watson MJ, Ye C, Ford BR, Lontos K, *et al.* Hypoxia drives CD39-dependent suppressor function in exhausted T cells to limit antitumor immunity. *Nature Immunology*. 2023; 24: 267–279. <https://doi.org/10.1038/s41590-022-01379-9>.
- [54] Guo Y, Xie YQ, Gao M, Zhao Y, Franco F, Wenes M, *et al.* Metabolic reprogramming of terminally exhausted CD8+ T cells by IL-10 enhances anti-tumor immunity. *Nature Immunology*. 2021; 22: 746–756. <https://doi.org/10.1038/s41590-021-00940-2>.
- [55] Guo Q. Targeting mitochondrial antioxidant MitoQ increases CD8+ memory T cell subsets in vitro. Master's thesis. Huazhong University of Science and Technology. 2022.
- [56] Fu YL, Zhou SN, Hu W, Li J, Zhou MJ, Li XY, *et al.* Metabolic interventions improve HBV envelope-specific T-cell responses in patients with chronic hepatitis B. *Hepatology International*. 2023; 17: 1125–1138. <https://doi.org/10.1007/s12072-023-10490-4>.